APPLICATION OF NUCLEAR METHODS

MEASUREMENT OF d(γ,p) REACTION CROSS SECTIONS AND ASYMMETRY WITH LINEARLY POLARIZED COHERENT BREMSSTRAHLUNG BEAM

G. Brudvik[1], D.D. Burdeinyi[2], V.B. Ganenko[2], K. Hansen[3], K. Fissum[3], L. Isaksson[3], K. Livingston[4], M. Lundin[1], B. Nilsson[1], B. Schröder[1,3]

[1]MAX-lab, Lund University, Lund, Sweden;

[2]National Science Center "Kharkov Institute of Physics and Technology", Kharkov, Ukraine;

[3]Department of Physics, Lund University, Lund, Sweden;

[4]Department of Physics and Astronomy, University of Glasgow, Glasgow, Scotland, UK

On the base of reaction of deuteron photo-disintegration it was studied possibility of the simultaneous measuring of cross sections and asymmetry of the (γ,p) reactions at the using of the coherent polarized photon beam. Measurements were performed for the proton emission angle 90°. The cross sections well agree with the literary data, obtained on the bremsstrahlung photon beam in the range of energies 45…80 MeV.

PACS: 03.65.Pm, 03.65.Ge, 61.80.Mk

INTRODUCTION

The (γ,p) reactions on nuclei are one of most studying photonuclear processes in the Giant Dipole Resonance and quasi-deuteron energy ranges. Up to now cross sections of these processes, measured with ordinary bremsstrahlung on some nuclei, represent main data array on this process, see, e.g. [1] and reference in there.

In the previous paper [2], the results on asymmetry of the carbon disintegration $^{12}C(\vec{\gamma},p)^{11}B$ have been presented in the intermediate energy range, obtained on polarized coherent bremsstrahlung (CB) photon beam

$$\Sigma=(d\sigma_{||}-d\sigma_{\perp})/(d\sigma_{||}+d\sigma_{\perp}), \quad (1)$$

where $d\sigma_{||(\perp)}\equiv d\sigma_{||(\perp)}/d\Omega$ is the reaction cross section for the photon polarization direction parallel (perpendicular) to the reaction plane. This observable value is important because it is determined through interference of the reaction amplitudes, thus some reaction mechanisms resulted from small amplitudes, which do not affect the reaction cross section, can be strengthened in this case. But the CB beam gives a possibility to get simultaneously data not only on the asymmetry, but also on the cross sections, because these observables are determined by the same values of the reaction yields.

The protons in the experiment [2] were detected by a ΔE-E CsI/SSD telescope consisted of two thick silicon strip detectors (SSDs) and a CsI(Tl) counter, and was not optimized for high energy resolution at the (γ,p) reaction measurements. The energy resolution of the missing energy spectra was ~3 MeV that did not allow to resolve the ground and excited states of the ^{11}B nucleus.

One of the ways of improvement its energy resolution it could be decreasing the kinematic broadening, if to use coordinate information of the detected events from the SSDs. Such possibility has been analyzed in [3] and it was found that resolution can be improved up to ~2.2…2.5 MeV, so more accurate data on the (γ,p) reactions can be obtained.

Thus, the goal of this work was, on the base of the deuteron photodisintegration reaction, to test methods on the (γ,p) reaction asymmetry and cross section measurements using the CB polarized photon beam, and to get more accurate data on these observables, using the strip information from the SSDs.

1. EXPERIMENTAL TECHNIQUE

The measurements have been performed at the MAX laboratory in Lund, described in Ref. [4] in details. The experimental set up, the CB beam production and characteristics, registration apparatus and technique have been described in Ref. [2 - 7] in details, thus only brief survey is given here.

The electron beam with energy E_0=192.7 MeV was extracted from the MAX-I storage ring, which worked in a stretcher mode. Then the beam was delivered into experimental area, shown in [2, 4 - 7], and was directed onto photon radiators, a diamond crystal of 100 μm thick and 50 μm Al foil, fixed in a target holder of the goniometer [6]. The beam size on the radiators was no more than 2 mm, and the electron current was ~5…10 nA. The duty cycle of the beam was df ≈ 50% and the divergence was no more 0.041° (~0.71 mrad) [6].

The post-bremsstrahlung electrons were detected by a focal plane (FP) hodoscope of the main tagger system [4]. The FP hodoscope provided 62 channels for detecting the post-bremsstrahlung electrons and total tagged energy range E_γ=21.9…78.8 MeV. The energy resolution smoothly varied from $\Delta E_\gamma \approx 0.8$ MeV till $\Delta E_\gamma \approx 1$ MeV [4, 6].

Photon beam collimator [4, 6, 7] was placed on the distance of ~214 cm from the photon radiators and had opening of 12 mm in diameter that provided the collimation angle $\theta_c \approx 1.2\theta_\gamma$ for a point-like electron beam ($\theta_\gamma=mc^2/E_0$ is the characteristic angle of bremsstrahlung, E_0 and m are the electron energy and mass).

The measurements were performed using a CD_2 plate of 1 mm thick, and a 1.1 mm CH_2 target for the carbon disintegration background subtraction. The targets were positioned on the distance ~2 m from the photon collimator at angle 60° to the photon beam direction.

Protons were detected by a CsI/SSD telescope [7], placed under angle θ_p= 90° to the beam axis. It consisted of two identical single-sided silicon strip detectors (SSDs) and a CsI(Tl) counter, which functioned as (ΔE)

and (E) detectors, respectively. The SSDs had a thickness of 0.5 mm and 64 strips, which were paralleled in groups of two for the read-out, thus yielding an effective strip width of 2 mm. The CsI(Tl) detector was of cylinder shape of 12.5 cm in diameter and 10 cm long. Its angular acceptance was determined by Monte Carlo simulation, using the GEANT-4 package, and was $\Delta\theta_p \approx \pm 14°$ (FWHM). The proton detection threshold was $T_{th} \approx 18$ MeV that corresponded to the photon energy of $E_\gamma \approx 40$ MeV for the d(γ,p)n reaction. The telescope was described in [7] in details.

2. POLARIZED PHOTON BEAM

Two runs have been produced with the polarized photon beam, which was generated at process of coherent bremsstrahlung of electrons in a diamond crystal. The crystal was orientated in such a way that main contribution to the CB cross section gave one vector of the reciprocal lattice of the crystal, [0 - 22] for parallel (PARA) and [0-2-2] for perpendicular (PERP) directions of the polarization to the reaction plane. The orientation angle values (the angles θ and α, defined in Ref. [6]) were taken that the CB peak energy was $E_{\gamma,d} \approx 51$ MeV in the Run-1, and $E_{\gamma,d} \approx 48$ MeV in the Run-2.

The crystal orientation was performed by a 3-axes goniometer assembled from five commercial moving stages. The goniometer construction, the crystal orientation methods and the CB beam spectral characteristics for various crystal orientations have been described in Ref. [6] in details.

2.1. CHARACTERISTICS OF NON-COLLIMATED COHERENT BREMSSTRAHLUNG BEAM

For determination the coherent beam characteristics and control their stability on-line measurements of the non-collimated CB spectra were performed by the FP hodoscope. They have shown that positions of the CB peak and the spectra shape were stable at the changing direction of the beam polarization within the measurements accuracy. However, there was a difference between counting rates of the odd and even FP channels, (as was discussed in [6, 7]), and in some cases it remained at the relative D/Al spectra, obtained by dividing the CB spectrum by the bremsstrahlung one from the Al radiator. Such difference in the D/Al spectra can be due to different background contributions to the FP detectors counting rate for the coherent and the bremsstrahlung spectra. In these cases, the D/Al spectra were averaged over neighboring FP channels.

The typical non-collimated D/Al spectra for the orientations being in the Run-1 are presented in Fig. 1. They demonstrate enhancement, or the, so-cold, coherent effect (the value of the relative spectrum in the CB maximum) $\beta \approx 1.35$, and a ~ 1 MeV difference of the CB peak positions for the PARA and PERP orientations.

The theoretical description of the spectra were performed by the ANB code [8], in which experimental factors, such as the electron beam divergence, beam spot size and multiple scattering in the crystal, the photon beam collimation were taken into account. At that, the angles of the crystal orientation (θ and α) and some constant background contribution to the incoherent part of the spectra were taken as the fitting parameters, values of which were determined by fitting the theoretical spectrum to the experimental one using a Fumili-2 algorithm [9]. The fit was performed because indication on the background contribution to the FP counting rate, as was noted the above, and necessity to specify the orientation angles values owing to possible changing of the "zero" angles [6] in the course of the measurements. The fit allowed one to describe more accurate the experimental spectra in all tagging energy interval, Fig. 1.

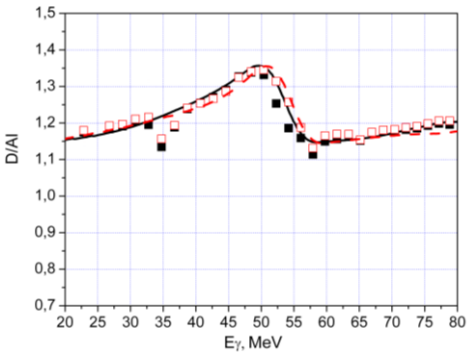

Fig. 1. Non-collimated relative D/Al spectra of the CB beam for Run-1 and the polarization direction parallel (full squares) and perpendicular (empty squares) to the reaction plane. Curves are results of the fit for the PARA (solid) and PERP (dashed) orientations, see text for details

The values of the orientation angles, obtained from the fit, coincided with the experimental values for the PERP orientations in both runs, but there was a ~ 10% difference between these values for the PARA orientations, perhaps owing to small change of the "zero" angle values. The background contribution to the FP detectors counting rate in the range of the CB peak was ~ 5…15% for both runs and orientations.

2.2. COLIMATED COHERENT BREMSSTRAHLUNG BEAM

The spectra and polarization of the CB beam, incident upon the nuclear target, were calculated by the ANB code, using the orientation angles values obtained by the fit, and taking into account the photon beam collimation and other experimental conditions, being in the Run-1 and 2. Results of the calculations are shown in Figs. 2 and 3.

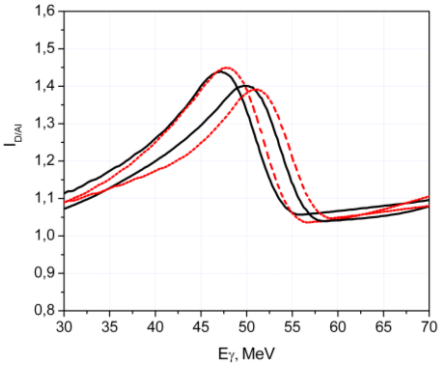

Fig. 2. Calculated D/Al spectra of the collimated ($\theta_c \approx 1.2\theta_\gamma$) coherent bremsstrahlung for PARA (solid lines) and PERP (dashed lines) orientations for Run-1 and Run-2 conditions

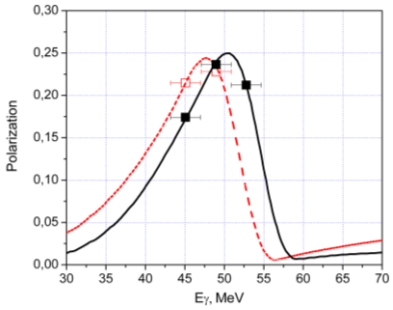

Fig. 3. Calculated polarization averaged over the PARA and PERP orientations, corresponding to the spectra, shown in Fig. 2, for Run-1 (solid line) and Run-2 (dashed). Points are the polarization averaged over energy bins, which were used for the asymmetry calculation, see text

The spectra for the PARA and PERP orientations for both runs have the similar shape and enhancement $\beta \approx 1.4…1.45$. But there is about ~1 MeV difference between the CB peak positions for the PARA and PERP orientations. Thus the calculated polarization for the PARA and PERP orientations was averaged. As can be seen in Fig. 3, the collimation increased the polarization value in the CB maxima till $P_\gamma \approx 0.25$ for both runs.

In order to increase statistics, summation of the reaction yields for four physically adjacent FP channels were produced, and twelve energy bins with the width $\Delta E_\gamma \approx 4$ MeV have been obtained (see below). Thus, polarization was averaged over the bin's width for the energy bins in the range of the CB maxima. For the asymmetry calculation only those bins were used, for which the polarization degree was $P_\gamma > 0.15$, as shown in Fig. 3.

3. DATA ANALYSIS

The analysis was divided into three parts. The first consists of selection protons from other particles, calculation their energy and energy of the photon, producing the reaction. The second part includes description of the background spectra generation, their subtraction, and extraction of the reaction yields. The third consists of determination experimental factors, such as solid angle, tagging efficiency, stolen corrections, and the cross sections and the beam asymmetry calculation. The first and some details of other parts of the analysis have been described in the previous work [7], in which the d(γ,p)n reaction cross sections measured on the non-polarized bremstrahlung beam has been analyzed.

3.1. PROTON IDENTIFICATION AND d(γ,p)n REACTION SELECTION

Protons were identified by standard ΔE−E method, based on relationship between energy losses ΔE and full energy E of the particles with different masses. The two-dimensional plot pairs of ADC signals from the SSD and the CsI detectors (see Fig. 3 in Ref. [7]) allowed to separate protons from other particles into clear band and to remove the background particles by special soft cut.

The stretched electron beam at the MAX-lab had a rather complicated time structure resulted from influence of the RF kicker magnet, used for extraction, and the incomplete filling of the ring during injection [4]. The coincidences between the SSDs and the CsI detector signals, corresponding to the proton band, generated trigger signals, which started the time measurements for all FP detectors. After correction of the trigger signals for time walk, a strong prompt peak of the time coincidence of the FP detectors and CsI/SSD telescope signals was obtained on top of random background in the individual tagger TDCs, see [7] for details. The time resolution of the FPtdc coincidence was ≈ 2…3 ns. In order to enable summing the FPtdc spectra, the prompt peaks for all FP channels were shifted to 750 channel of the FPtdc.

From the Gauss fit the position μ and the standard deviation σ of the peak were determined. The range μ±3σ defined the prompt region. It includes events both from reactions of the deuteron and the carbon disintegration, and the random background. The region to the right of the prompt peak includes only random events, which were taken for the background spectra generation.

A missing energy method was applied for selection the d(γ,p)n reaction and its yield obtaining. It assumes construction missing energy (MisE) spectra of the reaction under study, taking events from the prompt region of the FPtdc spectra. The missing energy is defined as

$$E_{mis}=E_\gamma-T_p-T_r, \qquad (2)$$

where E_γ is the photon energy, T_p is the proton kinetic energy in the reaction points, which is calculated using energy measured by the CsI detector, corrected to energy losses on the proton way from the origin point to the detector, T_r is the energy of a recoil nucleus (neutron in our case), which is calculated using the reaction kinematics, and values of the photon energy and the proton emission angle.

Each focal plane channel defines the deuteron disintegration reaction uncorrelated with the others. As was noted the above, summation of the MisE spectra for four physically adjacent FP channels was produced, in order to increase statistics. As a result, twelve MisE spectra have been obtained, corresponding to the energy bins with central energies E_γ = 37.2, 41.2, 45.1, 49.0, 52.8, 56.5, 60.2, 63.8, 67.3, 70.8, 74.3, 77.7 MeV and the bin's width, varying from $\Delta E_\gamma \approx 4$ till 3.4 MeV, respectively.

The missing energy spectra have typical shape for all bins and have been discussed in [7] in detail. There are maxima resulted from reactions of the carbon and deuteron (for measurements on the CD_2 target) disintegration, being on top of the random background. The peak corresponding to the deuteron disintegration is located at $E_{mis} \approx 2.2$ MeV for all bins. To the left side from the deuteron peak, there are maxima corresponding to reactions of the carbon disintegration. Firstly, the large peak, corresponding to reaction $^{12}C(\gamma,p)^{11}B$ when the recoil nucleus ^{11}B is in the ground state or in the first exited state with excitation energy E_{ex}= 2.12 MeV, secondly, the weaker peak resulted from sum of higher excited states of the ^{11}B with the E_{ex}= 5.02, 6.74, 6.79 and 7.29 MeV. These states are not resolved because of large energy resolution of the SSD/CsI telescope. To the left side from the carbon disintegration peaks there is the random background range.

Large energy resolution of the telescope, ~3 MeV (FWHM), was resulted from its construction, in which, firstly, there was much matter on the proton path (target,

SSDs, foils, etc.) that resulted in large ionization losses of the proton energy and their large fluctuations. Secondly, the telescope had angular acceptance $\Delta\theta_p \approx 28°$ (FWHM) [7] that caused kinematical broadening of the resolution, in the case of standard procedure of the data processing, when only ΔE information from the SSDs was taken into account. However, if to use coordinate information of the SSDs triggered strips, it is possible to separate the detected events into some groups, as a function of the proton emission angles that can be used for the recoil nuclei energy calculation at the MisE spectra construction.

Such approach has been developed in Ref. [3]. Seven groups of the events were formed from data array, for which the average angles of the proton emission varied from ~77° till 101°. Applying them for calculation the recoil neutron energy in (2) allowed one to improve the energy resolution in the MisE spectra to ~2.2…2.5 MeV.

3.2. THE RANDOM BACKGROUND SUBSTRACTION

As it was shown in Ref. [7], it was impossible to subtract, simultaneously and correctly, all background contribution to the deuteron maximum resulted from the carbon disintegration and the random coincidences, because of the random background was not identical for the CD_2 and the CH_2 spectra. Thus, two-step procedure was developed, which assumed two variants of its application, which differed by execution sequence of the random and the carbon background subtraction.

In the first variant (Variant A), on the first step the carbon background was removed by subtraction of the normalized the CH_2 MisE spectrum from the CD_2 one.

The remaining random background was small in the left side of the spectrum, below the deuteron peak, but reached ~ 10…20% under the peak [7]. On the second step, the remaining background, with the exception the deuteron peak range, was fitted by five order polynomial, which was subtracted from the spectrum. But this method was effective for energies $E_\gamma \geq 49.0$ MeV, for which energy interval to the right side from the deuteron peak is enough for the fitting.

In the second method (Variant B), on the first step, the random background was subtracted from the prompt missing energy spectra for both targets, CD_2 and CH_2, and, on the second step, the carbon background was removed by subtraction of the CH_2 MisE spectrum from the CD_2 one. Both methods have been used for data processing, both in previous [7] and in the present works, but if the Variant A was used without changing, for the Variant B more accurate procedure of the random background spectra normalization was applied.

The background spectra were generated for both targets taking events from the random range of the corresponding TDC spectra (Fig. 4 in the Ref. [7]). At that, there are two conditions, which should be controlled. Firstly, the generated and the prompt background spectra should have the same (or very close) energy dependence, in order to get full random background subtraction after the spectra normalization. Secondly, the resulting CD_2 and CH_2 spectra after the random background subtraction have to coincide in the energy interval to the right side of the d(γ,p) peak, where contributions from reactions of the carbon disintegration are identical for both targets, and should be canceled at the CD_2 and CH_2 spectra subtraction.

Normalization coefficients for the generated background spectra were obtained from analysis of energy dependences of the prompt and the generated background spectra ratios, because they are more convenient for the above requirements control. Typical behavior of the ratios as function of E_{mis} energy are shown in Fig. 4 for the spectra, corresponding to the CD_2 and CH_2 targets and photon energies E_γ=(49.0±1.9) MeV. They demonstrate maxima of the deuteron and the two-body carbon disintegration, discussed the above. To the left from the carbon disintegration maxima there is a range, where the ratios oscillate around practically constant values (see left and middle panels in Fig. 4).

Three missing energy intervals were considered in this range to test the difference of the background spectra energy dependences: the whole interval (A) from some E_{mis} bins above left end of the spectrum (where statistics is very small) till left side of the carbon peak; two, approximately equal, right (B) and left (C) parts of the interval A. In the case shown in Fig. 4, these intervals are: A= –36.25…–8.65 MeV, B= –26.65…–8.65 MeV, and C= –36.25…–23.95 MeV. Average values of the ratios in these intervals were calculated

$$k_{A,B,C}=\sum(N_{p,i}/N_{r,i})/N_{A,B,C}, \quad (3)$$

where $N_{p,i}$ and $N_{r,i}$ are values of the events in the i-th missing energy bin of the prompt and random spectra, $N_{A,B,C}$ is the total number of the events in the intervals A, B, C, respectively. The difference in the coefficients $k_{A,B,C}$ values represents difference of the energy dependences of the generated and prompt random background.

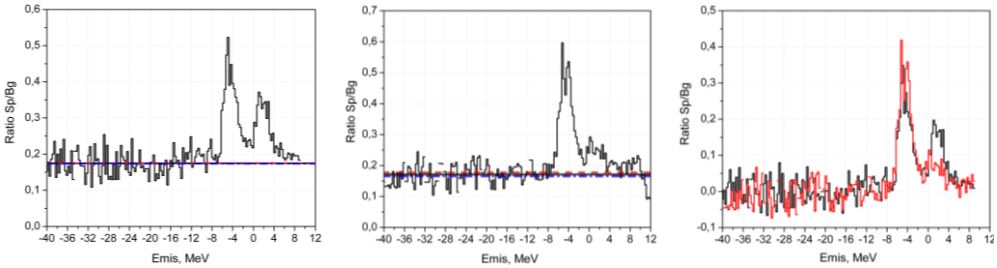

Fig. 4. Ratios of the prompt and the random background spectra as a function of missing energy for CD_2 (left) and CH_2 (middle) targets for Run-1 and PARA orientation. Lines correspond to normalization coefficient values for CD_2 and CH_2 spectra, respectively: k_{AD}=0.17469 and k_{AH}=0.17123 (solid), k_{BD}=0.17547 and k_{BH}=0.17768 (dashed), k_{CD}=0.17345 and k_{CH}=0.16534 (dash-dotted). Right: the ratios after the background subtraction using coefficients k_{AD} and k_{BH}. Photon energy bin E_γ=(49.0±1.9) MeV

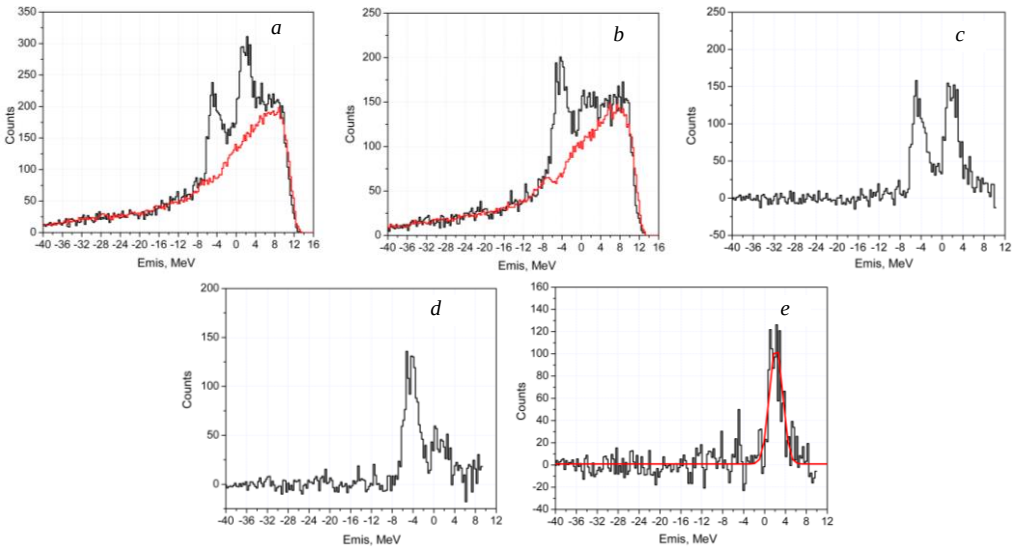

Fig. 5. Missing energy spectra of the protons for the CD_2 (a) and CH_2 (b) targets for Run-1 and PARA orientation and simulated random background spectra after normalization; (c) and (d) are the above spectra after the random background subtraction; (e) is the d(γ,p)n reaction missing energy spectrum after the CD_2 and CH_2 spectra subtraction. Line is the Gauss fit. Photon energy bin E_γ=(49.0±1.9) MeV

Usually, these normalization coefficients were close, e.g., in Fig. 4 (left), where their values differ ~1% that is less of their errors (~2...2.5%). Thus, they give practically identical results at the background subtraction. In some cases the difference between coefficients was more, as in the case shown in Fig. 5 (middle), where it reaches ~7%. In such cases some variants of the normalization coefficients were considered, and those of them were taken for normalization, which gave closer CD_2 and CH_2 MisE spectra in the range above the d(γ,p) peak after the background subtraction. For the spectra in Fig. 5, this is coefficients k_{AD} and k_{BH}. They provide the background subtraction that satisfies the above second criterion, as shown in the Fig. 5 (right). These coefficients were used for normalization the generated random background spectra. Sequential steps of the background subtraction from the prompt CD_2 and CH_2 spectra till final d(γ,p)n MisE spectra, are shown in Fig. 5. Such procedure was applied for all energy bins.

3.3. THE REACTION YIELD DETERMINATION

The reaction yields were obtained from the d(γ,p)n MisE spectra, such as shown in Fig. 5,e, by two ways. Firstly, by fit the d(γ,p) peak by Gaussian and calculation its square, and secondly, by summation events in the peak region, μ±3σ, where μ and σ are the peak position and standard deviation taken from the Gauss fit. The yields coincided with a good accuracy independently of the beam run and crystal orientation.

The variants A and B of the data processing gave also close yield values, and statistical error of the yields for both variants was mainly determined by the number of counts, N_{CD} and N_{CH}, in the prompt peaks of the CD_2 and CH_2 spectra, $\Delta Y_p \approx (N_{CD}+N_{CH})^{1/2}$, because in the case of the Variant A, the remaining background was small, usually no more ~10% of the sum $N_{CD}+N_{CH}$, and in the case of the Variant B, accuracy of the generated background was high enough, see [7] for details.

The yields were obtained for 10 energy bins for the Run 1 and 2, starting from the bin E_γ = (45.1±2) MeV, because of threshold of the d(γ,p)n reaction detection by the telescope, $E_{\gamma,th} \approx$ 40 MeV. The statistical accuracy of the yields varied from ~10% at E_γ =(45.1±2) MeV to ~20% for E_γ =(77.6±1.7) MeV.

4. CROSS SECTIONS CALCULATION

The d(γ,p)n reaction differential cross sections were obtained using the formula,

$$d\sigma/d\Omega=(Y_{p,||}/N_{\gamma,||}\varepsilon_{st,||}+Y_{p,\perp}/N_{\gamma,\perp}\varepsilon_{st,\perp})/2N_D\Delta\Omega, \quad (4)$$

where $Y_{p,||(\perp)}$, $\varepsilon_{st||(\perp)}$, $N_{\gamma,||(\perp)}$ are the reaction yield, the stolen correction, the photon flux incident on the target, respectively, corresponding to the PARA (PERP) orientations of the photon beam polarization.

The photon flux is determined by the relation,

$$N_{\gamma,||(\perp)}=N_e'_{||(\perp)}\varepsilon_{CBtag}, \quad (5)$$

where $N_e'_{||(\perp)}$ is the number of the post-bremsstrahlung electrons, detected by the FP detectors at the PARA (PERP) orientations, and ε_{CBtag} is the CB beam tagging efficiency. The tagging efficiency and the stolen corrections calculations are presented below.

The number of deuteron nuclei per cm^2 and the effective solid angle value of the CsI/SSD telescope have been determined in Ref. [7], there values are $N_D=1.541\cdot10^{22}$ D/cm^2 and ΔΩ=(249.00±2.25) msr.

4.1. STOLEN CORRECTION

This correction resulted from the fact that the uncorrelated electron can be registered in the region to the left of the prompt peak, thus a focal plane TDC can be stopped by a random electron, arriving earlier than a correlated one. The stolen correction is determined by the counting rates in the focal-plane detectors and the beam duty factor. If the random events are Poisson distributed in time, this correction may be written as [10]

$$\varepsilon_{st,i}=\exp(-t_0 n_{FP,i}/df), \quad (6)$$

where $n_{FP,i}$ is the counting rate, corresponding to the FP channel (i), t_0 is the position of the lower limit of the prompt region in the FPtdc spectrum, df is the average duty factor of the beam. The values of the duty factor (df = 0.5) and the t_0 position ($t_0 \approx$ 128.1 ns) were used

the same as in [7]. The counting rate per focal plane channel ranged from ~1.2 till 0.4 MHz with increasing energy of the bin. For the PARA and PERP orientations they were close for both runs and were averaged. The stolen corrections were practically identical for CD_2 and CH_2 measurements for both runs, and depend on photon energy, changing from ~30% at E_γ=45 MeV till ~14% at E_γ=78 MeV.

4.2. TAGGING EFFICIENCY

The photon beam tagging efficiency was measured for the collimator hole of 12 mm in diameter both for the bremsstrahlung beam, produced from the 50 μm Al, and for the CB beam from the 100 μm diamond crystal at the CB peak energy $E_{\gamma,d}\approx$ 60 MeV [11].

In the case of the bremsstrahlung beam the tagging efficiency was ε_{tag}=0.350±0.002 within interval $E_\gamma\approx$ 50…80 MeV. Results of the simulation by GEANT-4 code [7] have given also constant value of the tagging efficiency in this energy interval, but ~6.8% more than the experimental value, $\varepsilon_{tag,m}$=0.374±0.002. Such difference may be due to ~6% background contribution to the FP detectors counting rate that agrees with estimation, obtained at the non-collimated CB spectra fit.

Because angular dependences of the coherent and incoherent parts of the CB radiation are different, the CB beam tagging efficiency differs from that of the bremsstrahlung. The measurements [11] have shown that it was alike the CB spectrum by the shape, it had maximum at the CB peak energy, and plane decreased with the energy decreasing, but sharply decreased above the peak, and was practically constant at the energy increasing, because influence of the coherent part of the radiation becomes insignificant.

In order to estimate the tagging efficiency for the crystal orientations, being in the Run-1 and 2, the ratios of the CB collimated and non-collimated relative D/Al spectra were calculated for these orientations

$$R_{D/Al}=Sp(D/Al)_{col}/Sp(D/Al)_{no}. \quad (7)$$

It relates the CB and the bremsstrahlung beams tagging efficiencies

$$\varepsilon_{CBtag}=\varepsilon_{tag}R_{D/Al}. \quad (8)$$

The calculated tagging efficiency was ~7.5% more than the measured one in the energy range behind the CB peak that may be due to the same reason, as discussed the above. Thus the calculated tagging efficiency was normalized to the experimental value [11] in high energy range. The tagging efficiencies for the PARA and PERP orientations were, practically, identical, thus they were averaged. The results are presented in Fig. 6.

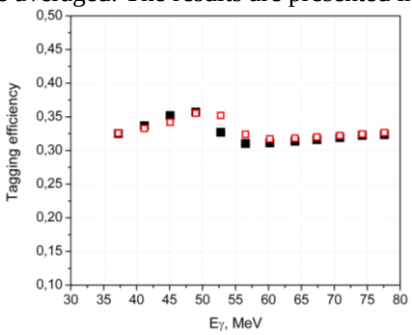

Fig. 6. The coherent bremsstrahlung beam tagging efficiency for the Run-1 (empty squares) and the Run-2 (full squares), averaged for the PARA and PERP orientations

5. CROSS SECTIONS RESULTS

The differential cross sections of the d(γ, p) reaction are presented in Fig. 7, for two variants (A and B) of the data processing. There are some conclusions from the data analysis.

1) The cross sections calculated using the reaction yields, obtained by summation of the events under deuteron peak and by Gauss fit of the peak were practically identical in all energy interval, Fig. 7,a.

2) The cross sections obtained by variants A and B of the data processing, in a whole, have coincided within the data accuracy for both runs, Figs. 7,a and 7,b. But at the more detailed consideration, the cross sections obtained by the Variant A were slightly systematic below than the cross sections, obtained by the Variant B, ~3 and ~6.5% for the Run-1 and Run-2, respectively. At that, the Variant B gives the cross sections, which better agree with the literature data in all energy range. However, the measurements on the bremsstrahlung beam [7], on the contrary, demonstrate that the cross sections obtained by the Variant A were ~10% higher the cross sections obtained by the Variant B.

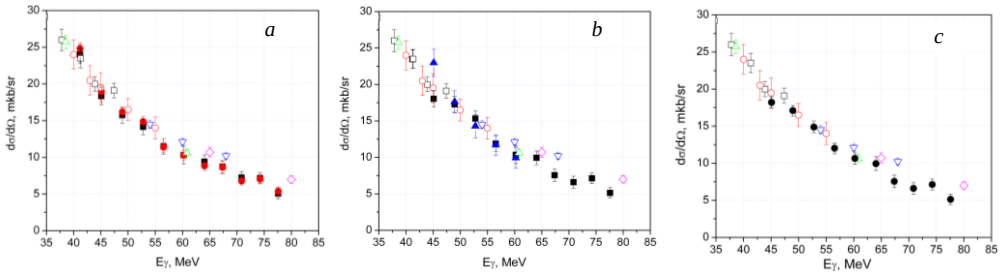

Fig. 7. Differential cross sections of the d(γ,p) reaction for proton emission angle θ_p=90° obtained by: a) variant-A of the Run-1 data processing, the yields obtained by summation the events in the deuteron peak (full squares) and by the Gauss fit the deuteron peak (circles); b) variant-B of the Run-1 data processing. Full triangles are cross sections obtained in [7] with the bremsstrahlung beam; c) variant-B of the data processing, averaged over Run-1 and 2 (full circles). The reaction yield is obtained by summation events in the deuteron peak. Literature data: [12] – empty squares, [13] – triangles down, [14] – triangles, [15] – empty circles, [16] – rhombus

One of possible reason of such differense of the cross sections may be due to inaccuracy of the residual background fitting in the Variant A of the data processing, resulted from small statistics in the region above the peak of deuteron disintegration after the MisE CD_2 and CH_2 spectra subtraction. In general, the Variant

B gives more stable results, thus it is more preferable and is used in further.

3) A comparison of the cross sections obtained with the bremsstrahlung and the coherent bremsstrahlung beams was carried out in the CB peak region, where their spectra were essentially different. As can be seen in Fig. 7,b, the cross sections well agree in this region, the average value of their ratios is 0.98 ± 0.05.

The cross sections measured in the Run-1 and 2 practically coincided within the data accuracy and have been averaged. The results are presented in Fig. 7,c. They well agree with the literature data in whole energy interval of the measurements E_γ=45…78 MeV.

Systematic uncertainty includes errors due to solid angle, resulted from uncertainties of the measurements of the set up dimensions (2%), the stolen correction due to uncertainties of the beam duty factor value (5%) and tagging efficiency, resulted from uncertainties due to the background contribution (6%). Thus, the root mean square of the systematic uncertainties was ~8%, under the assumption of independent sources.

6. CROSS SECTION ASYMMETRY

The cross section asymmetry was calculated using the same the d(γ, p) reaction yields, $Y_{p,||(\perp)}$,

$$\Sigma=(Y_{p,||}-Y_{p,\perp})/(Y_{p,||}+Y_{p,\perp})/P_\gamma, \quad (9)$$

where P_γ is the photon polarization, calculated in the section 1.4. The asymmetry was calculated for the energy bins in the range of the CB maximum, for which the polarization degree was $P_\gamma \geq 0.15$ (as shown in Fig. 3). This condition restricted the asymmetry calculation by three bins for the Run-1 with central energies, E_γ=45.1, 49.0 and 52.8 MeV, and two bins for the Run-2 with E_γ=45.1 and 49.0 MeV. Because the asymmetry values had large statistical errors, due to low polarization and small statistics, they have been averaged over energy for each run. The obtained values of the asymmetry are Σ= (0.68±0.12) at E_γ= (47±4) MeV, and Σ=(0.51±0.13) at E_γ= (49±6) MeV, and shown in Fig. 8. The results agree with existing data within the data accuracy. Systematic uncertainty includes error mainly due to photon polarization determination, because of relative character of this observable, and was ~ 8 and 6% for the above asymmetry values, respectively.

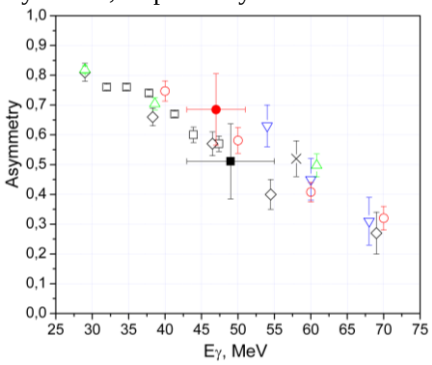

Fig. 8. Asymmetry of the d(γ,p)n reaction for proton emission angle θ_p=90°, measured in Run-1 (full squares) and Run-2 (full circles). Empty squares are data [12], triangles down – [13], triangles – [14], rhombus – [17], circles – [18], crosses – [19]

SUMMARY

Measurements of the reaction of the deuteron disintegration d(γ,p)n have been performed at the MAX-laboratory, with aim to test possibility of the (γ,p) reactions asymmetry and the cross sections measurements using the coherent polarized photon beam. The protons were detected by the ΔE-E telescope, placed under angle 90° to the photon beam direction. For the reaction identification a missing energy method was applied. The energy resolution of the telescope has been improved by reducing the kinematic broadening, due to using of information on the coordinates of the detected events from the silicon strip detectors that makes it possible to get more accurate missing energy spectra.

Two methods of the data processing were tested, which differed by execution sequence of the random and the carbon background subtraction.

The second method (Variant B) which assumes subtraction of the random background from the CD_2 and CH_2 MisE spectra, on the first step, and applying the difference method, on the second step gives more stable results, which better agrees with the literature data.

The differential cross sections and the asymmetry of the d(γ,p) reaction have been obtained for proton emission angle θ_p=90° in the energy intervals $E_\gamma \approx$ 45…78 and 45…53 MeV, respectively. The cross sections well agree with the literature data, obtained on the ordinary bremsstrahlung beam. Within the data accuracy the asymmetry agrees also with the literature data, although accuracy of the asymmetry is not high due to poor statistics. On the whole, the measurements with the coherent bremsstrahlung photon beam allow one to get information on the cross section and asymmetry on the (γ,p) reactions on nuclei, simultaneously.

REFERENCES

1. H. Ruijter, J.-O. Adler, K. Hansen, et al. // *Phys. Rev.* 1996, v. C54, p. 3076.
2. D. Burdeinyi, J. Brudvik, K. Fissum, et al. // *Nuclear Physics*. 2017, v. A957, p. 321-331.
3. G. Brudvik, D. Burdeinyi, V. Ganenko, et al. Improvement of energy resolution of ΔE-E CsI/SSD-Telescope at Measurement of (γ,p)-reactions using strip information of SSD // *Problems of Atomic Science and Technology. Series "Nuclear Physics Investigations"*. 2016, №3, p. 111.
4. J.-O. Adler, M. Boland, J. Brudvik, et al. // *Nucl. Instr. and Meth*. 2013, v. A715, p. 1-10.
5. V. Ganenko, K. Fissum, K. Hansen, et al. // *Problems of Atomic Science and Technology. Series "Nuclear Physics Investigations"*. 2009, №3, p. 95-102.
6. V. Ganenko, J. Brudvik, D. Burdeinyi, et al. // *Nucl. Instr. and Meth.* 2014, v. A763, p. 137-149.
7. G. Brudvik, D. Burdeinyi, V. Ganenko, et al. // *Problems of Atomic Science and Technology*. 2015, №3.
8. F.A. Natter et al. // *Nucl. Instr. and Meth*. 2003, v. B211, p. 465-486.
9. https://root.cern.ch/numerical-minimization
10. R.O. Owens // *Nucl. Instr. and Meth*. 1990, v. A288, p. 574.

11. J. Brudvik et al. Summary of the MAX-lab Run Period 2008.04.14 - 2008.04.28.
12. D. Babusci, V. Bellini, M. Capogni, et al. // *Nucl. Phys.* 1998, v. A633, p. 683-694.
13. K.-H.Krause, J.Sobolewski, J.Ahrens, et al. // *Nucl. Phys.* 1992, v. A 549, p. 387-406.
14. M.P. De Pascale, G. Giordano, G. Matone, et al. // *Phys. Rev*. 1985, v. C 32, p. 1830.
15. B. Weissman and H.L. Schultz // *Nucl. Phys.* 1971, v. A1 74, p. 129.
16. E. Whalin, B. Dwight Schriever, A. Hanson // *Phys. Rev*. 1956, v. 101.
17. W. Del Bianco, L. Federici, G. Giordano, et al. // *Phys. Rev. Lett.* 1981, v. 47, p. 1118.
18. В.П. Баранник, В.Г. Горбенко, В.А. Гущин и др. // *Ядерная физика*. 1983, т. 38, с. 1108.
19. И.Е. Внуков, И.В. Главанаков, Ю.Ф. Кречетов и др. // *Ядерная физика*. 1988, т. 47, с. 913.

Article received 16.01.2018

ИЗМЕРЕНИЕ АСИММЕТРИИ И СЕЧЕНИЯ РЕАКЦИИ d(γ,p) НА ПОЛЯРИЗОВАННОМ КОГЕРЕНТНО-ТОРМОЗНОМ ПУЧКЕ

G. Brudvik, Д.Д. Бурдейный, В.Б. Ганенко, K. Hansen, K. Fissum, L. Isaksson, K. Livingston, M. Lundin, B. Nilsson, B. Schröder

На примере реакции фотодезинтеграции дейтрона исследована возможность одновременного измерения сечений и асимметрии (γ,p)-реакций при использовании когерентного поляризованного пучка фотонов. Измерения проведены для угла вылета протона 90°. Сечения хорошо согласуются с литературными данными, полученными на тормозном пучке фотонов в диапазоне энергий 45…80 МэВ.

ВИМІРЮВАННЯ АСИМЕТРІЇ ТА ПЕРЕРІЗУ РЕАКЦІЇ d(γ,p) НА ПОЛЯРИЗОВАНОМУ КОГЕРЕНТНО-ГАЛЬМІВНОМУ ПУЧКУ

G. Brudvik, Д.Д. Бурдейный, В.Б. Ганенко, K. Hansen, K. Fissum, L. Isaksson, K. Livingston, M. Lundin, B. Nilsson, B. Schröder

На прикладі реакції фотодезинтеграції дейтрона досліджена можливість одночасного вимірювання перетинів і асиметрії (γ,p)-реакції при використанні когерентного поляризованого пучка фотонів. Вимірювання виконані для кута вильоту протонів 90°. Перетини добре узгоджуються з літературними даними, отриманими на гальмівниму пучку фотонів у діапазоні енергій 45…80 МеВ.